Circulation: Cardiovascular Imaging

ORIGINAL ARTICLE

Radiotracer Imaging Allows for Noninvasive Detection and Quantification of Abnormalities in Angiosome Foot Perfusion in Diabetic Patients With Critical Limb Ischemia and Nonhealing Wounds

See Editorial by Finn and Lawrence

Jessica L. Alvelo, MD
Xenophon Papademetris, PhD
Carlos Mena-Hurtado, MD
Sangchoon Jeon, PhD
Bauer E. Sumpio, MD, PhD
Albert J. Sinusas, MD
Mitchel R. Stacy, PhD

BACKGROUND: Single photon emission computed tomography (SPECT)/computed tomography (CT) imaging allows for assessment of skeletal muscle microvascular perfusion but has not been quantitatively assessed in angiosomes, or 3-dimensional vascular territories, of the foot. This study assessed and compared resting angiosome foot perfusion between healthy subjects and diabetic patients with critical limb ischemia (CLI). Additionally, the relationship between SPECT/CT imaging and the ankle–brachial index—a standard tool for evaluating peripheral artery disease—was assessed.

METHODS AND RESULTS: Healthy subjects (n=9) and diabetic patients with CLI and nonhealing ulcers (n=42) underwent SPECT/CT perfusion imaging of the feet. CT images were segmented into angiosomes for quantification of relative radiotracer uptake, expressed as standardized uptake values. Standardized uptake values were assessed in ulcerated angiosomes of patients with CLI and compared with whole-foot standardized uptake values in healthy subjects. Serial SPECT/CT imaging was performed to assess uptake kinetics of technetium-99m-tetrofosmin. The relationship between angiosome perfusion and ankle–brachial index was assessed via correlational analysis. Resting perfusion was significantly lower in CLI versus healthy subjects (P=0.0007). Intraclass correlation coefficients of 0.95 (healthy) and 0.93 (CLI) demonstrated excellent agreement between serial perfusion measurements. Correlational analysis, including healthy and CLI subjects, demonstrated a significant relationship between ankle–brachial index and SPECT/CT (P=0.01); however, this relationship was not significant for diabetic CLI patients only (P=0.2).

CONCLUSIONS: SPECT/CT imaging assesses regional foot perfusion and detects abnormalities in microvascular perfusion that may be undetectable by conventional ankle–brachial index in patients with diabetes mellitus. SPECT/CT may provide a novel approach for evaluating responses to targeted therapies.

Key Words: diabetes mellitus ■ ischemia ■ perfusion imaging ■ peripheral artery disease

http://circimaging.ahajournals.org

CLINICAL PERSPECTIVE

Peripheral artery disease is an atherosclerotic disease of the lower extremities that is highly prevalent in patients with diabetes mellitus, who commonly present with both macrovascular and microvascular complications. These disruptions to the microcirculation contribute to high rates of foot ulceration and poor rates of treatment success and limb salvage in patients with diabetes mellitus. Lower extremity revascularization procedures, such as stenting, balloon angioplasty, and surgical bypass, are used to target areas of the foot that are ischemic and contain nonhealing wounds. Angiosomes, which are 3-dimensional vascular territories that have been defined based on specific upstream source arteries, can assist in the guidance of targeted revascularization strategies; however, no standard imaging approach exists for assessing microvascular perfusion within downstream vascular territories of the foot that are targeted for revascularization. In the present study, we demonstrate that radiotracer-based imaging with single photon emission computed tomography (SPECT)/CT offers a noninvasive approach for assessing regional differences in microvascular foot perfusion between healthy control subjects and diabetic patients with critical limb ischemia and is also capable of detecting focal perfusion defects in regions of foot ulceration. Additionally, we show that SPECT-derived perfusion values do not significantly correlate with the ankle–brachial index, which suggests that SPECT/CT imaging may offer improved sensitivity over conventional peripheral artery disease screening tools. Future application of this SPECT/CT imaging approach may allow for improved assessment of the diabetic foot, as well as offer novel insight into revascularization procedures and other therapeutic interventions targeted at restoring perfusion to specific angiosomes of the foot.

Peripheral artery disease (PAD) is a progressive atherosclerotic disease of the lower limbs that affects 8 to 10 million Americans[1] and is more prevalent and progresses more quickly in patients with diabetes mellitus (DM).[2,3] Microvascular disease is highly prevalent in patients with DM, who commonly present with both microvascular and macrovascular complications that are also accompanied with accelerated endothelial dysfunction, atherosclerosis, and cardiovascular disease.[4,5] These disruptions to the microcirculation may play a significant role in high rates of lower extremity ulceration and an impaired wound healing process that exists in the setting of DM.[6,7] Critical limb ischemia (CLI), which is defined by ischemic rest pain or the presence of a nonhealing arterial ulcer or gangrene of the foot, is an advanced and debilitating form of PAD that commonly manifests in the setting of DM and is associated with high incidence of lower extremity amputation.[8] Therefore, prompt treatment of the diabetic foot with revascularization procedures, such as stenting, balloon angioplasty, and surgical bypass, can be critical for improving rates of wound healing and reducing the need for future amputations.

During the last 30 years, the concept of the angiosome—a 3-dimensional (3D) vascular territory supplied by a specific source artery—has evolved and advanced the way in which vascular teams are planning revascularization strategies to target ischemic nonhealing foot ulcers.[9] The angiosome concept, first described by Taylor and Palmer in 1987,[10] divides the foot and ankle into downstream 3D territories that are supplied by the upstream anterior tibial, posterior tibial, and peroneal arteries. Clinical trials comparing direct (angiosome guided) to indirect (nonangiosome) revascularization have demonstrated that angiosome-guided revascularization of the lower extremities can result in significantly faster wound healing,[11–13] higher rates of wound healing,[14] and improvement in overall limb salvage outcomes in patients with PAD.[11,12,15] Additionally, recent meta-analysis further suggests a reduced risk of major extremity amputation in patients with PAD undergoing revascularization using an angiosome-guided approach.[16]

Current clinical imaging tools have limitations related to assessment of microvascular disease in patients with PAD and are commonly restricted to evaluating microvascular perfusion within superficial tissue or only allow for evaluation of major vessel blood flow and morphology.[17] Although magnetic resonance-based approaches, such as blood oxygen level dependent,[18,19] arterial spin labeling,[20,21] and contrast-enhanced imaging,[22] are capable of quantifying 3D tissue oxygenation and perfusion, these approaches do not allow for assessment of resting foot perfusion and generally require exercise, pharmacological, or reactive hyperemia paradigms to produce quantifiable signals. Radiotracer-based perfusion imaging with single photon emission computed tomography (SPECT)/computed tomography (CT) offers some advantages over conventional imaging techniques by allowing for serial volumetric assessment of regional microvascular perfusion in the lower extremities under resting conditions without the need for iodine- or gadolinium-based contrast agents.[23]

In this study, we present a CT-based image segmentation approach for evaluation of resting microvascular perfusion within specific foot angiosomes using hybrid SPECT/CT imaging. Additionally, we assess the relationship between SPECT/CT perfusion imaging and a standard clinical tool for evaluating PAD (the ankle–brachial index [ABI]), as well as utilize a previously developed

image registration technique[19,24] for evaluating potential variability in the uptake of technetium-99 m (^{99m}Tc)-tetrofosmin in the DM foot for optimization of lower extremity SPECT/CT perfusion imaging. We hypothesized that SPECT/CT imaging under resting conditions would allow for assessment and identification of abnormalities in microvascular perfusion within angiosomes of the foot in diabetic patients with CLI. We also hypothesized that SPECT/CT perfusion imaging would not be significantly correlated to ABI measures in diabetic patients with microvascular disease because of the ABI being limited to only arterial assessment, whereas SPECT perfusion offers a more comprehensive assessment of both the macrovasculature and microvasculature.

METHODS

The data, analytic methods, and study materials will not be made available to other researchers for purposes of reproducing the results or replicating the procedure.

Research Subjects

Subject recruitment included healthy subjects (n=9) and diabetic patients with CLI (n=42). A medical history was taken before subject enrollment to evaluate each subject's risk factors for cardiovascular, pulmonary, and metabolic disease, which included history of DM, smoking, hypertension, hypercholesterolemia, and family history of coronary artery disease. Patients with DM were considered to have CLI based on the presence of a nonhealing foot ulcer or resting pain in the foot or calf, as well as history of abnormal ABI (<0.9 or ≥1.3). Additional inclusion criteria for patients with DM included patients ≥18 years of age with previously diagnosed type II DM, based on any of the following criteria: fasting plasma glucose >126 mg/dL on 2 separate occasions, HbA_{1c} (glycated hemoglobin) ≥6.5%, and 2-hour plasma glucose ≥200 mg/dL in an oral glucose tolerance test. Exclusion criteria included patients <18 years of age, HbA_{1c} <6.5%, concurrent enrollment in another clinical trial, and cognitive deficiencies that would impair the ability to provide informed consent. Patients were not eliminated from enrollment consideration because of common diabetic foot conditions, such as cellulitis, osteomyelitis, Charcot foot, and stasis dermatitis.

Healthy control subjects were recruited using a research flyer and screened using a standard medical history questionnaire. Healthy subjects were void of PAD, DM, coronary artery disease, cancer, hypertension, and smoking history. To ensure that healthy subjects were absent of PAD and hypertension, all subjects underwent screening that included measurement of ABI in both lower extremities and assessment of resting brachial artery blood pressure.

The study protocol was approved by the Yale University Institutional Review Board for Human Subjects Research and Review Committee and the Radiation Safety Committee and was in accordance with the guidelines set forth by the Declaration of Helsinki. All individuals provided written informed consent after receiving an explanation of the experimental procedures and potential risks associated with participating in the study.

SPECT/CT Clinical Imaging Protocol

Subjects reported for SPECT/CT imaging after an 8-hour fast that also consisted of abstinence from caffeine and alcohol. All patients and healthy volunteers underwent resting SPECT/CT imaging at the level of the ankle and foot using a conventional hybrid SPECT/4-slice CT imaging system with large field-of-view NaI detectors and general purpose parallel-hole collimators (Infinia Hawkeye; GE Healthcare). All subjects received a low-dose (547.7±47.9 MBq) intravenous injection of ^{99m}Tc-tetrofosmin under resting conditions and underwent SPECT imaging 15 minutes after radiotracer injection. SPECT images were acquired using a 360° step and shoot acquisition with a 140.5 keV±10% window, 3° projections, and 30 seconds per stop. Immediately after the SPECT acquisition, CT images were acquired with a slice thickness of 5 mm, at 140 kVp, and 2.5 mA for the purposes of attenuation correction and future image segmentation of foot angiosomes. All SPECT images were reconstructed using iterative reconstruction, applying corrections for attenuation, scatter, and resolution loss. SPECT/CT images were reconstructed using system software (Xeleris; GE Healthcare, Buckinghamshire, United Kingdom) capable of generating coregistered functional (SPECT) and anatomic (CT) images of the feet. SPECT images were reconstructed and fused with CT attenuation images for quantification of perfusion within specific angiosomes of the foot.

For optimization of the ideal SPECT/CT imaging time point after radiotracer injection, and for assessing any potential delay in the uptake of ^{99m}Tc-tetrofosmin in foot tissue in the setting of PAD, a subset of healthy subjects (n=8) and patients with DM (n=6) underwent serial SPECT/CT image acquisitions at both 15 and 45 minutes after ^{99m}Tc-tetrofosmin injection using identical image acquisition and reconstruction parameters as described above.

SPECT/CT Image Processing

SPECT/CT images were analyzed using a previously developed image analysis toolkit (BioImage Suite, http://www.bioimagesuite.org) for regional assessment of lower extremity tissue perfusion,[23,25] oxygenation,[19,26] and angiogenesis.[27] Low-dose CT attenuation images were used to segment and define angiosomes of the feet (lateral plantar, medial plantar, lateral calcaneal, medial calcaneal, and dorsal foot; Figure 1). Average radiotracer uptake was assessed from coregistered SPECT images within the CT-defined 3D angiosome containing the nonhealing ulcer. Average SPECT image intensity values were normalized to injected radiotracer dose (mCi) and patient body weight (kg) to generate standardized uptake values. In healthy volunteers who did not have foot ulceration, average SPECT activity was assessed across the entire 3D volume of the foot from the subject's dominant leg.

In subjects who underwent SPECT/CT perfusion imaging at 15 and 45 minutes after radiotracer injection, serial images were coregistered utilizing a previously published automated approach of image registration to ensure precise analysis of perfusion within the same 3D image space over time.[19,24] Specifically, the image registration approach utilizes a 2-step process of global rigid alignment followed by nonrigid image registration that ultimately corrects for

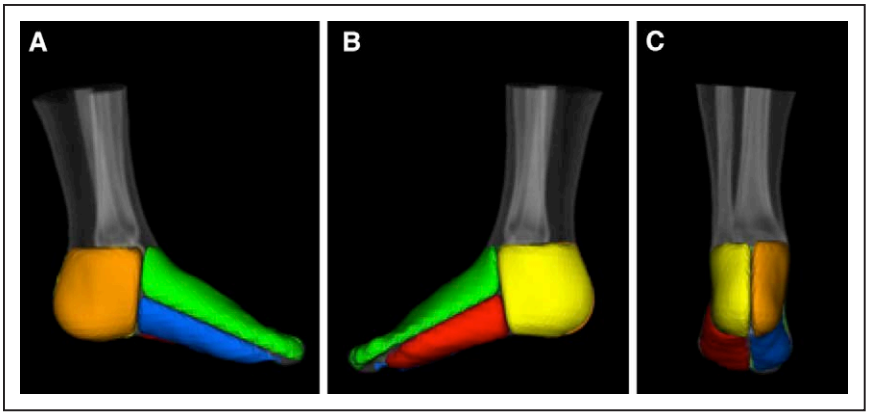

Figure 1. Volume rendered foot angiosomes overlaid on X-ray computed tomography attenuation images acquired in a patient with critical limb ischemia. **A**, Medial, (**B**) lateral, and (**C**) posterior views display the medial heel (orange), lateral heel (yellow), dorsal foot (green), medial plantar (blue), and lateral plantar (red) angiosomes.

any changes in foot position that may occur between image acquisitions (Figure 2).

Measurement of ABI

The ABI was assessed in healthy and DM subjects by manual measurement of the systolic blood pressure from both brachial arteries, as well as from both the dorsalis pedis and posterior tibial arteries, after a minimum of 10-minute rest in the supine position. Pressures were measured using a standard blood pressure cuff and a handheld 8-MHz Doppler probe (Dopplex D900; ArjoHuntleigh, Inc, Addison, IL). All pressures were acquired by the same experienced investigator to limit variability between subjects. ABI measurements were acquired in all healthy subjects (n=9) and a subset of diabetic patients with CLI (n=30).

Statistical Analysis

Unpaired *t* tests were used to compare baseline demographics between healthy subjects and diabetic patients with CLI, and general linear model was used to identify differences in baseline SPECT perfusion values (standardized uptake values) between healthy and CLI groups after controlling for age. Serial SPECT measurements acquired at 15 and 45 minutes post-radiotracer injection were assessed for the discrepancy and the consistency of the repeated 2 measures using Bland–Altman plot and intraclass correlation coefficient (ICC), respectively. Pearson correlation coefficient was used to assess the relationship between resting SPECT perfusion values and ABI measurements. Normality was assessed for all continuous variables using the Kolmogorov–Smirnov test. All statistical analyses were performed using commercially available software (GraphPad Prism v7.0 for Mac OS X; GraphPad Software, La Jolla, CA; SAS/STAT v9.4 for Windows; SAS Institute, Inc, Cary, NC). Statistical significance for all analyses was set at $P<0.05$. All values are expressed as means±SD unless stated otherwise.

RESULTS

Subject Demographics

Medical history questionnaires, along with ABI and blood pressure screening, confirmed that all healthy subjects were void of cardiovascular, metabolic, and pulmonary disease and did not have significant risk factors for cardiovascular disease. Alternatively, all patients with CLI had previously diagnosed type II DM (HbA_{1c}, 8.7±2.1%) and presented with numerous cardiovascular comorbidities, which included hypertension (92.9% of patients with CLI), hyperlipidemia (66.7%), coronary artery disease (52.4%), renal disease (35.7%), prior stroke (21.4%), and history of tobacco use (64.3%). Additionally, several enrolled patients with CLI presented with Charcot foot (n=3), stasis dermatitis (n=6), osteomyelitis (n=2), and cellulitis (n=2). Diabetic patients with CLI also presented with significantly reduced ABI values when compared with healthy subjects (healthy, 1.05±0.1; patients with CLI, 0.63±0.2; $P<0.0001$). No statistically significant differences existed between subject groups for body mass index (healthy, 27.5±3.7; patients with CLI, 29.9±6.4; $P=0.3$), systolic blood pressure (healthy, 123.8±14.0; patients with CLI, 136.6±20.4; $P=0.1$), and diastolic blood pressure (healthy, 76.5±9.9; patients with CLI, 71.4±12.0; $P=0.3$). However, significant differences in age existed between healthy subjects and patients with CLI (healthy, 49.7±9.7; patients with CLI, 67.0±12.7; $P=0.0003$).

Comparison of Resting Foot Perfusion Between Healthy Subjects and Patients With CLI

Qualitative analysis of ^{99m}Tc-tetrofosmin SPECT/CT images demonstrated the ability to noninvasively detect resting perfusion defects in sites containing nonhealing foot ulcers in patients with CLI (Figure 3). Further application of lower extremity SPECT/CT imaging in both healthy subjects and patients with CLI demonstrated the capability of identifying qualitative (Figure 4A through 4C) and quantitative (Figure 4D) differences in microvascular foot perfusion between subject groups under resting conditions. The 2 subject groups had unequal variances ($F=4.37$; $P=0.03$), and the mean difference of SPECT perfusion between groups was significantly different

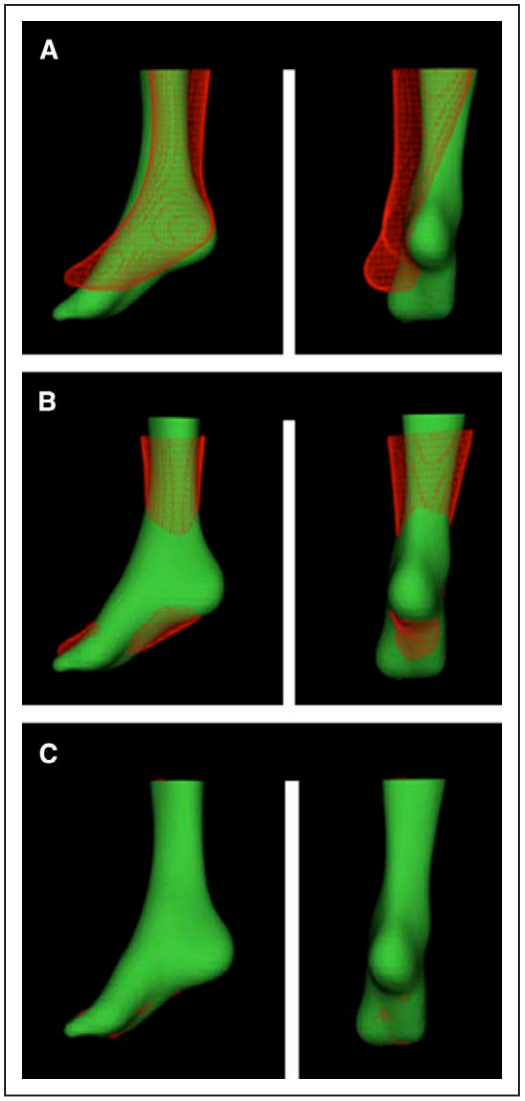

Figure 2. Serial registration of x-ray computed tomography foot images for assessing test–retest reliability of single photon emission computed tomography/CT perfusion imaging.
Registration was achieved using points from outer skin surfaces. Pictured are lateral and posterior views of rendered surfaces from 2 separate imaging studies (green, scan 1 foot position; and red, scan 2 foot position) at the (**A**) starting position before registration, (**B**) after global rigid registration, and (**C**) after nonrigid registration.

(*P*=0.0007) by unpaired *t* test with the Satterthwaite approximation for degree of freedom. By eliminating 1 outlier in the CLI patient group that was responsible for the unequal variance, the mean difference between groups was still significant (*P*=0.003) with a pooled SD. Additionally, the group differences in SPECT perfusion remained statistically significant after controlling for age (*P*=0.01), with age-adjusted means of 0.23 (SE=0.025) and 0.15 (SE=0.01) in healthy subjects and patients with CLI, respectively.

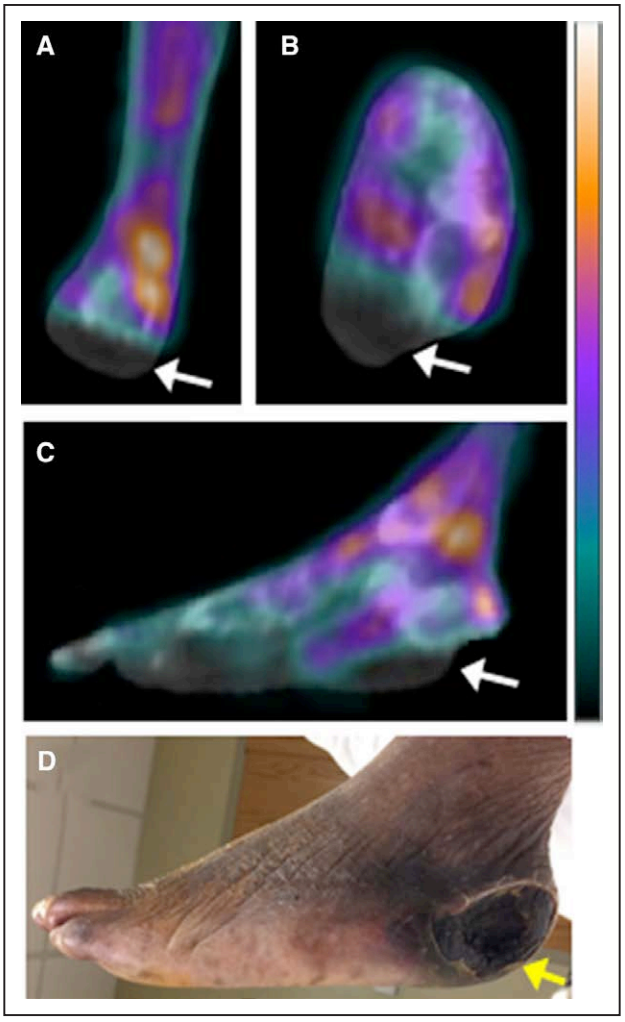

Figure 3. Resting ^{99m}Tc-tetrofosmin single photon emission computed tomography (SPECT)/computed tomography (CT) perfusion imaging in a critical limb ischemia patient with a nonhealing foot ulcer.
A, Coronal, (**B**) axial, and (**C**) sagittal views of fused SPECT/CT images reveal a relative perfusion defect (denoted by white arrows) located in the (**D**) region of the nonhealing wound (denoted by yellow arrow) that extends along the plantar aspect of the foot.

Assessment of Uptake Kinetics of ^{99m}Tc-Tetrofosmin in Diabetic CLI

The Bland–Altman plot (Figure 5) displays the difference between 2 serial tests (test 1–test 2) against the mean perfusion values measured for all foot angiosomes. The mean differences for patients with CLI (mean, 0.000; 95% confidence interval, –0.004 to 0.003) and healthy subjects (mean, 0.008; 95% confidence interval, 0.006–0.011) is also displayed. The 95% limits of agreement were –0.018 to 0.018 and –0.008 to 0.024 in patients with CLI and healthy subjects, respectively. The ICCs of >0.99 obtained in all angiosomes represent an excellent consistency of SPECT/CT perfusion imaging values acquired at 15 and 45 minutes post-radiotracer

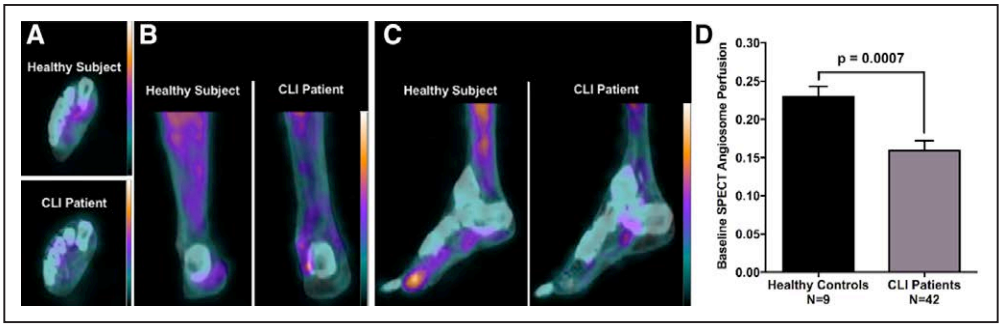

Figure 4. Comparison of resting single photon emission computed tomography (SPECT)/computed tomography (CT) perfusion imaging in healthy and critical limb ischemia (CLI) subjects.
A, Axial, (**B**) coronal, and (**C**) sagittal views of ^{99m}Tc-tetrofosmin SPECT/CT imaging demonstrate visual differences in foot perfusion under resting conditions. **D**, Quantitative image analysis reveals significant differences in resting foot perfusion (standardized uptake values) between healthy subjects and patients with CLI.

injection. After controlling for each angiosome region, ICC values in both healthy subjects (ICC=0.946) and patients with CLI (ICC=0.929) demonstrated a strong level of agreement.

Relationship Between SPECT/CT Perfusion Imaging and ABI

The relationship between SPECT/CT perfusion imaging and ABI was assessed under resting, baseline conditions. Correlational analysis, including both diabetic patients with CLI and healthy subjects, demonstrated a significant and positive relationship between SPECT-derived angiosome foot perfusion and the ABI

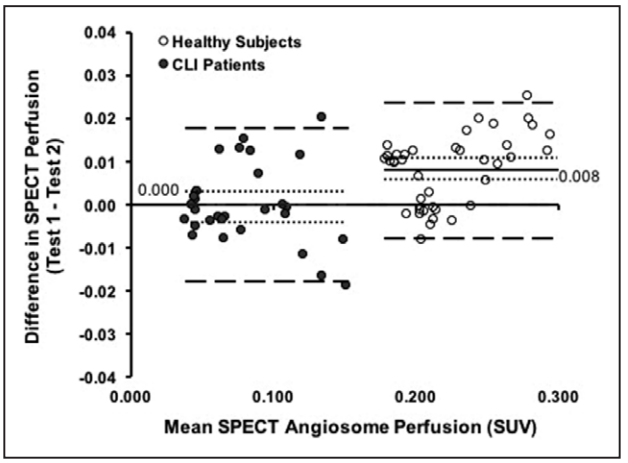

Figure 5. Evaluation of ^{99m}Tc-tetrofosmin uptake kinetics in the feet of healthy subjects and patients with critical limb ischemia (CLI).
The Bland–Altman plot collectively displays perfusion values for each angiosome in healthy and CLI subjects. Intraclass correlation coefficients of 0.95 (healthy subjects) and 0.93 (patients with CLI) demonstrated excellent agreement level between measurements acquired at 15 and 45 min post-radiotracer injection. n=8 healthy subjects, and n=6 patients with CLI. SPECT indicates single photon emission computed tomography; and SUV, standardized uptake value.

(*r*=0.41, *P*=0.01; Figure 6A). However, individual correlational analysis of SPECT and ABI measures specifically within the diabetic CLI patient population did not demonstrate a significant relationship (*r*=0.25, *P*=0.19; Figure 6B).

DISCUSSION

In the present study, we demonstrate for the first time the application of radiotracer-based imaging for the quantitative assessment of microvascular perfusion within specific angiosomes of the foot by using a CT-based image segmentation approach and serial image registration. We also demonstrate that SPECT/CT imaging of the foot is a useful noninvasive technique that allows for detection of regional abnormalities in resting microvascular perfusion in the setting of DM and CLI, as well as quantifiable differences in perfusion between diabetic patients with CLI and healthy subjects. Additionally, we show that in the setting of DM, SPECT/CT imaging of microvascular perfusion is not significantly correlated with the ABI—a standard clinical tool for assessing large-vessel PAD.

Early research studies that applied gamma cameras for the assessment of PAD were primarily accomplished by 2-dimensional scintigraphy or used thallium-201, without assessing regional variability in perfusion within specific 3D vascular territories.[17] However, PAD-focused research in the past decade has begun to use the ^{99m}Tc-labeled perfusion tracers ^{99m}Tc-tetrofosmin and ^{99m}Tc-sestamibi, which has reduced radiation exposure to patients, increased image quality on gamma cameras, and demonstrated clinical utility in the detection of PAD within the calf,[28,29] as well as assisted with tracking the response to cell therapy in the foot.[30–32] Additionally, recent preclinical research has established and validated methods for assessing serial changes in microvascular perfusion within specific lower extremity muscle groups using SPECT/CT imaging.[23] The present study represents the next step in translation

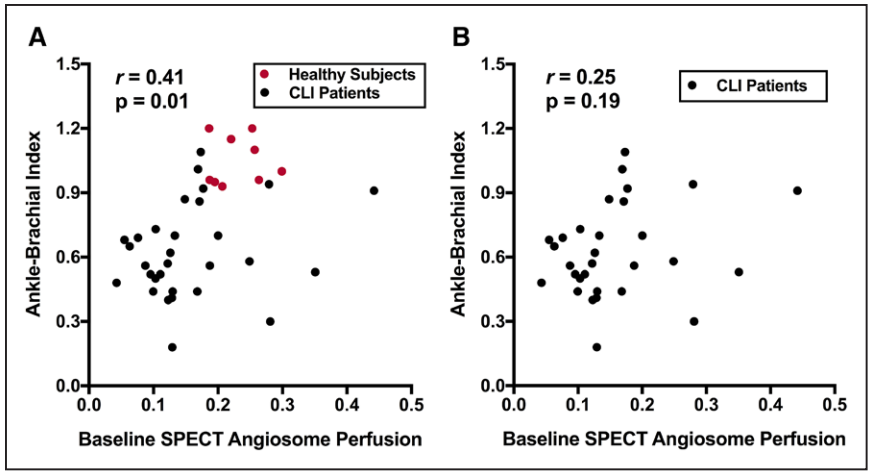

Figure 6. Evaluation of the relationship between single photon emission computed tomography (SPECT)-derived angiosome perfusion and ankle–brachial index (ABI).
A, Correlational analysis of both healthy and critical limb ischemia (CLI) subjects demonstrated a significant relationship between ABI and SPECT angiosome perfusion; however, this relationship was not significant in (**B**) correlational analysis of patients with CLI only. n=30 patients with CLI, and n=9 healthy subjects.

of this SPECT/CT perfusion imaging approach into a DM patient population at high risk for lower extremity amputation. Our findings that demonstrate the repeatability of quantitative analysis of regional foot perfusion at 15 and 45 minutes post-radiotracer injection suggests that SPECT/CT perfusion imaging can be performed in patients with PAD early or late post-injection without any significant effect on perfusion results. SPECT/CT imaging of angiosome foot perfusion may have significant clinical implications by offering a novel approach for evaluating the response to targeted revascularization procedures in the lower extremities, which could assist interventionalists who are attempting to target and increase perfusion within specific ulcerated regions of the foot in an effort to facilitate wound healing and limb salvage. Additionally, SPECT/CT perfusion imaging performed under baseline conditions may possess value by characterizing viable from nonviable foot tissue in patients with CLI, which could potentially offer guidance when the location and level of amputation is under consideration. Although the present work was limited to the setting of CLI, the ability to identify both qualitative and quantitative abnormalities within specific angiosomes of the foot under resting conditions may also offer future clinical value by detecting subtle abnormalities in perfusion that precede the development of claudication or the formation of ulcers in patients across the entire clinical spectrum of PAD. It should also be noted that although the present work used ^{99m}Tc-tetrofosmin for SPECT/CT perfusion imaging, ^{99m}Tc-sestamibi has also demonstrated utility for detection of PAD in prior studies and could, therefore, serve as an alternative to ^{99m}Tc-tetrofosmin in future preclinical and clinical investigations.[28,29,33]

The lack of a significant relationship between SPECT/CT-derived measures of angiosome perfusion and the ABI is not surprising because prior ABI-focused publications have demonstrated that limitations of ABI include artificially elevated values in the presence of noncompressible arteries and the inability to detect microvascular disease,[34] both of which being highly prevalent in the setting of DM. Additionally, because of ABI consisting of assessing arterial pressures at the level of the arm and ankle, SPECT/CT imaging, which reflects both proximal macrovascular disease, as well as microvascular perfusion in the foot, should inherently offer a more sensitive approach for noninvasively assessing localized abnormalities in the microcirculation of patients with DM. Indeed, prior radiotracer-based investigations have demonstrated that perfusion imaging of the calf on gamma cameras is more sensitive than ABI[35] and Doppler ultrasound[28,36] for identifying abnormalities in calf microvascular perfusion in both asymptomatic[35,36] and symptomatic[28] patients, which suggests that lower extremity SPECT/CT perfusion imaging may be capable of detecting subtle changes in skeletal muscle physiology in the early stages of PAD that could go undetected by conventional ABI. Although SPECT/CT perfusion imaging and ABI were not significantly correlated, characterization of the relationship between these noninvasive tools should clarify how our novel imaging approach may fit into the screening paradigm for PAD, which includes ABI measurement.[37] Additionally, even though current guidelines for CLI suggest assessment of toe pressures, transcutaneous oxygen pressure, or skin perfusion pressure for evaluating microvascular disease and wound healing potential,[8] these tools remain limited to superficial evaluation of perfusion or do not allow for 3D assessment of perfusion within specific foot angiosomes. The findings from the present study associated with the use of SPECT/CT imaging for evaluation of tissue perfusion within 3D foot angiosomes suggest that radiotracer-based imaging may possess potential for improving the baseline assessment of microvascular disease in patients with PAD, which is particularly relevant to patients with DM and CLI.

LIMITATIONS

Although the present study demonstrated use of SPECT/CT imaging for the assessment of angiosome foot perfusion, the total number of enrolled patients was relatively small. Therefore, wider application of lower extremity SPECT/CT perfusion imaging is warranted to validate the findings of this study and fully assess the diagnostic utility of this imaging approach in the setting of PAD. Additionally, although we evaluated the relationship between SPECT/CT perfusion imaging and ABI in the current work, future work should also assess the relationship between SPECT/CT imaging and other metrics of perfusion, such as the toe–brachial index and transcutaneous oxygen pressure, to fully understand the clinical relevance of our imaging approach. In the present study, we used a conventional NaI SPECT camera for all imaging. With the recent development of cadmium–zinc–telluride SPECT cameras that have demonstrated potential for quantitative assessment of myocardial perfusion and absolute myocardial blood flow,[38,39] future investigations translating cadmium–zinc–telluride technology to the lower extremities may allow for improved quantitative analysis of skeletal muscle physiology. Future work focused on SPECT/CT imaging of foot perfusion may also benefit by additional evaluation of all foot angiosomes to understand how impaired microvascular perfusion within a specific ulcerated angiosome may influence perfusion in other angiosomes of the foot.

CONCLUSIONS

Collectively, the present study demonstrates that ^{99m}Tc-tetrofosmin SPECT/CT imaging is a useful tool for assessing regional foot perfusion and can detect abnormalities in resting microvascular perfusion that may be undetectable by conventional ABI in the setting of DM. Future application of angiosome-based SPECT/CT perfusion imaging across the broader clinical spectrum of PAD may provide novel insight into the response to targeted revascularization, surgical bypass, and novel cell- or gene-based therapies directed at improving tissue perfusion or promoting angiogenesis within ischemic tissue of the lower extremities that is susceptible to future wound formation and amputation.

ARTICLE INFORMATION

Received July 14, 2017; accepted February 22, 2018.

Correspondence

Mitchel R. Stacy, PhD, Center for Regenerative Medicine, The Research Institute at Nationwide Children's Hospital, 700 Children's Drive, WB4131, Columbus, OH 43205. Email: mitchel.stacy@nationwidechildrens.org

Affiliations

Department of Internal Medicine (J.L.A., C.M.-H., B.E.S., A.J.S., M.R.S.), Department of Radiology and Biomedical Imaging (X.P., B.E.S., A.J.S.), Department of Biomedical Engineering (X.P.), Yale School of Nursing (S.J.), and Department of Surgery (B.E.S.), Yale University School of Medicine, New Haven, CT.

Acknowledgments

We would like to acknowledge all of the nuclear medicine technologists within the Nuclear Cardiology Laboratory at Yale New Haven Hospital who provided technical assistance with single photon emission computed tomography/computed tomography imaging.

Sources of Funding

This work was supported, in part, by National Institutes of Health grant R01 HL135103 (Dr Stacy) and American Heart Association award No. 14CRP20480404 (Dr Stacy).

Disclosures

None.

REFERENCES

1. Leeper NJ, Kullo IJ, Cooke JP. Genetics of peripheral artery disease. *Circulation*. 2012;125:3220–3228. doi: 10.1161/CIRCULATIONAHA.111.033878.
2. Norgren L, Hiatt WR, Dormandy JA, Nehler MR, Harris KA, Fowkes FG; TASC II Working Group. Inter-society consensus for the management of peripheral arterial disease (TASC II). *J Vasc Surg*. 2007;45(suppl S):S5–S67. doi: 10.1016/j.jvs.2006.12.037.
3. Peach G, Griffin M, Jones KG, Thompson MM, Hinchliffe RJ. Diagnosis and management of peripheral arterial disease. *BMJ*. 2012;345:e5208.
4. Forbes JM, Cooper ME. Mechanisms of diabetic complications. *Physiol Rev*. 2013;93:137–188. doi: 10.1152/physrev.00045.2011.
5. Saad MI, Abdelkhalek TM, Saleh MM, Kamel MA, Youssef M, Tawfik SH, Dominguez H. Insights into the molecular mechanisms of diabetes-induced endothelial dysfunction: focus on oxidative stress and endothelial progenitor cells. *Endocrine*. 2015;50:537–567. doi: 10.1007/s12020-015-0709-4.
6. Hicks CW, Selvarajah S, Mathioudakis N, Perler BA, Freischlag JA, Black JH III, Abularrage CJ. Trends and determinants of costs associated with the inpatient care of diabetic foot ulcers. *J Vasc Surg*. 2014;60:1247, 1254.e1–1254, 1254.e1. doi: 10.1016/j.jvs.2014.05.009.
7. Bowling FL, Rashid ST, Boulton AJ. Preventing and treating foot complications associated with diabetes mellitus. *Nat Rev Endocrinol*. 2015;11:606–616. doi: 10.1038/nrendo.2015.130.
8. Kinlay S. Management of Critical Limb Ischemia. *Circ Cardiovasc Interv*. 2016;9:e001946. doi: 10.1161/CIRCINTERVENTIONS.115.001946.
9. Manzi M, Cester G, Palena LM, Alek J, Candeo A, Ferraresi R. Vascular imaging of the foot: the first step toward endovascular recanalization. *Radiographics*. 2011;31:1623–1636. doi: 10.1148/rg.316115511.
10. Taylor GI, Palmer JH. The vascular territories (angiosomes) of the body: experimental study and clinical applications. *Br J Plast Surg*. 1987;40:113–141.
11. Lejay A, Georg Y, Tartaglia E, Gaertner S, Geny B, Thaveau F, Chakfe N. Long-term outcomes of direct and indirect below-the-knee open revascularization based on the angiosome concept in diabetic patients with critical limb ischemia. *Ann Vasc Surg*. 2014;28:983–989. doi: 10.1016/j.avsg.2013.08.026.
12. Huang TY, Huang TS, Wang YC, Huang PF, Yu HC, Yeh CH. Direct revascularization with the angiosome concept for lower limb ischemia: a systematic review and meta-analysis. *Medicine (Baltimore)*. 2015;94:e1427. doi: 10.1097/MD.0000000000001427.
13. Sumpio BE, Forsythe RO, Ziegler KR, van Baal JG, Lepantalo MJ, Hinchliffe RJ. Clinical implications of the angiosome model in peripheral vascular disease. *J Vasc Surg*. 2013;58:814–826. doi: 10.1016/j.jvs.2013.06.056.
14. Iida O, Takahara M, Soga Y, Yamauchi Y, Hirano K, Tazaki J, Yamaoka T, Suematsu N, Suzuki K, Shintani Y, Miyashita Y, Uematsu M. Impact of angiosome-oriented revascularization on clinical outcomes in critical limb ischemia patients without concurrent wound infection and diabetes. *J Endovasc Ther*. 2014;21:607–615. doi: 10.1583/14-4692R.1.
15. Iida O, Soga Y, Hirano K, Kawasaki D, Suzuki K, Miyashita Y, Terashi H, Uematsu M. Long-term results of direct and indirect endovascular revas-

cularization based on the angiosome concept in patients with critical limb ischemia presenting with isolated below-the-knee lesions. *J Vasc Surg*. 2012;55:363.e5–370.e5. doi: 10.1016/j.jvs.2011.08.014.
16. Bosanquet DC, Glasbey JC, Williams IM, Twine CP. Systematic review and meta-analysis of direct versus indirect angiosomal revascularisation of infrapopliteal arteries. *Eur J Vasc Endovasc Surg*. 2014;48:88–97. doi: 10.1016/j.ejvs.2014.04.002.
17. Stacy MR, Sinusas AJ. Novel applications of radionuclide imaging in peripheral vascular disease. *Cardiol Clin*. 2016;34:167–177. doi: 10.1016/j.ccl.2015.06.005.
18. Bajwa A, Wesolowski R, Patel A, Saha P, Ludwinski F, Ikram M, Albayati M, Smith A, Nagel E, Modarai B. Blood oxygenation level-dependent CMR-derived measures in critical limb ischemia and changes with revascularization. *J Am Coll Cardiol*. 2016;67:420–431. doi: 10.1016/j.jacc.2015.10.085.
19. Stacy MR, Qiu M, Papademetris X, Caracciolo CM, Constable RT, Sinusas AJ. Application of BOLD magnetic resonance imaging for evaluating regional volumetric foot tissue oxygenation: a feasibility study in healthy volunteers. *Eur J Vasc Endovasc Surg*. 2016;51:743–749. doi: 10.1016/j.ejvs.2016.02.008.
20. Grözinger G, Pohmann R, Schick F, Grosse U, Syha R, Brechtel K, Rittig K, Martirosian P. Perfusion measurements of the calf in patients with peripheral arterial occlusive disease before and after percutaneous transluminal angioplasty using MR arterial spin labeling. *J Magn Reson Imaging*. 2014;40:980–987. doi: 10.1002/jmri.24463.
21. Pollak AW, Meyer CH, Epstein FH, Jiji RS, Hunter JR, Dimaria JM, Christopher JM, Kramer CM. Arterial spin labeling MR imaging reproducibly measures peak-exercise calf muscle perfusion: a study in patients with peripheral arterial disease and healthy volunteers. *JACC Cardiovasc Imaging*. 2012;5:1224–1230. doi: 10.1016/j.jcmg.2012.03.022.
22. Jiji RS, Pollak AW, Epstein FH, Antkowiak PF, Meyer CH, Weltman AL, Lopez D, DiMaria JM, Hunter JR, Christopher JM, Kramer CM. Reproducibility of rest and exercise stress contrast-enhanced calf perfusion magnetic resonance imaging in peripheral arterial disease. *J Cardiovasc Magn Reson*. 2013;15:14. doi: 10.1186/1532-429X-15-14.
23. Stacy MR, Yu DY, Maxfield MW, Jaba IM, Jozwik BP, Zhuang ZW, Lin BA, Hawley CL, Caracciolo CM, Pal P, Tirziu D, Sampath S, Sinusas AJ. Multimodality imaging approach for serial assessment of regional changes in lower extremity arteriogenesis and tissue perfusion in a porcine model of peripheral arterial disease. *Circ Cardiovasc Imaging*. 2014;7:92–99. doi: 10.1161/CIRCIMAGING.113.000884.
24. Papademetris X, Jackowski AP, Schultz RT, Staib LH, Duncan JS. Computing 3D non-rigid brain registration using extended robust point matching for composite multisubject fMRI analysis. *Med Image Comput Comput Assist Interv*. 2003;2879:788–795.
25. Stacy MR, Zhou W, Sinusas AJ. Radiotracer imaging of peripheral vascular disease. *J Nucl Med*. 2013;54:2104–2110. doi: 10.2967/jnumed.112.115105.
26. Stacy MR, Caracciolo CM, Qiu M, Pal P, Varga T, Constable RT, Sinusas AJ. Comparison of regional skeletal muscle tissue oxygenation in college athletes and sedentary control subjects using quantitative BOLD MR imaging. *Physiol Rep*. 2016;4:e12903.
27. Dobrucki LW, Dione DP, Kalinowski L, Dione D, Mendizabal M, Yu J, Papademetris X, Sessa WC, Sinusas AJ. Serial noninvasive targeted imaging of peripheral angiogenesis: validation and application of a semiautomated quantitative approach. *J Nucl Med*. 2009;50:1356–1363. doi: 10.2967/jnumed.108.060822.
28. Soyer H, Uslu I. A patient with peripheral arterial stenosis diagnosed with lower extremity perfusion scintigraphy. *Clin Nucl Med*. 2007;32:458–459. doi: 10.1097/RLU.0b013e318059b54a.
29. Kuśmierek J, Dabrowski J, Bieńkiewicz M, Szumiński R, Płachcińska A. Radionuclide assessment of lower limb perfusion using 99mTc-MIBI in early stages of atherosclerosis. *Nucl Med Rev Cent East Eur*. 2006;9:18–23.
30. Takagi G, Miyamoto M, Fukushima Y, Yasutake M, Tara S, Takagi I, Seki N, Kumita S, Shimizu W. Imaging angiogenesis using 99mTc-macroaggregated albumin scintigraphy in patients with peripheral artery disease. *J Nucl Med*. 2016;57:192–197. doi: 10.2967/jnumed.115.160937.
31. Miyamoto M, Yasutake M, Takano H, Takagi H, Takagi G, Mizuno H, Kumita S, Takano T. Therapeutic angiogenesis by autologous bone marrow cell implantation for refractory chronic peripheral arterial disease using assessment of neovascularization by 99mTc-tetrofosmin (TF) perfusion scintigraphy. *Cell Transplant*. 2004;13:429–437.
32. Takagi G, Miyamoto M, Tara S, Takagi I, Takano H, Yasutake M, Tabata Y, Mizuno K. Controlled-release basic fibroblast growth factor for peripheral artery disease: comparison with autologous bone marrow-derived stem cell transfer. *Tissue Eng Part A*. 2011;17:2787–2794. doi: 10.1089/ten.tea.2010.0525.
33. Hendrikx G, Vries MH, Bauwens M, De Saint-Hubert M, Wagenaar A, Guillaume J, Boonen L, Post MJ, Mottaghy FM. Comparison of LDPI to SPECT perfusion imaging using (99m)Tc-sestamibi and (99m)Tc-pyrophosphate in a murine ischemic hind limb model of neovascularization. *EJNMMI Res*. 2016;6:44. doi: 10.1186/s13550-016-0199-2.
34. Shishehbor MH, White CJ, Gray BH, Menard MT, Lookstein R, Rosenfield K, Jaff MR. Critical limb ischemia: an expert statement. *J Am Coll Cardiol*. 2016;68:2002–2015. doi: 10.1016/j.jacc.2016.04.071.
35. Duet M, Virally M, Bailliart O, Kevorkian JP, Kedra AW, Benelhadj S, Ajzenberg C, Le Dref O, Guillausseau PJ. Whole-body (201)Tl scintigraphy can detect exercise lower limb perfusion abnormalities in asymptomatic diabetic patients with normal Doppler pressure indices. *Nucl Med Commun*. 2001;22:949–954.
36. Celen YZ, Zincirkeser S, Akdemir I, Yilmaz M. Investigation of perfusion reserve using 99Tc(m)-MIBI in the lower limbs of diabetic patients. *Nucl Med Commun*. 2000;21:817–822.
37. Brownrigg JR, Schaper NC, Hinchliffe RJ. Diagnosis and assessment of peripheral arterial disease in the diabetic foot. *Diabet Med*. 2015;32:738–747. doi: 10.1111/dme.12749.
38. Wells RG, Timmins R, Klein R, Lockwood J, Marvin B, deKemp RA, Wei L, Ruddy TD. Dynamic SPECT measurement of absolute myocardial blood flow in a porcine model. *J Nucl Med*. 2014;55:1685–1691. doi: 10.2967/jnumed.114.139782.
39. Feher A, Sinusas AJ. Quantitative assessment of coronary microvascular function. Dynamic single-photon emission computed tomography, positron emission tomography, ultrasound, computed tomography, and magnetic resonance imaging. *Circ Cardiovasc Imaging*. 2017;10:e006427.

Radiotracer Imaging Allows for Noninvasive Detection and Quantification of Abnormalities in Angiosome Foot Perfusion in Diabetic Patients With Critical Limb Ischemia and Nonhealing Wounds

Jessica L. Alvelo, Xenophon Papademetris, Carlos Mena-Hurtado, Sangchoon Jeon, Bauer E. Sumpio, Albert J. Sinusas and Mitchel R. Stacy

Circ Cardiovasc Imaging. 2018;11:
doi: 10.1161/CIRCIMAGING.117.006932
Circulation: Cardiovascular Imaging is published by the American Heart Association, 7272 Greenville Avenue, Dallas, TX 75231

Print ISSN: 1941-9651. Online ISSN: 1942-0080